

PHYSICAL REVIEW B

SOLID STATE

THIRD SERIES, VOL. 3, NO. 6

15 MARCH 1971

Electrical Properties of Amorphous Se, As_2Se_3 , and As_2S_3

A. I. Lakatos and M. Abkowitz

Xerox Corporation, Research Laboratories, Rochester, New York 14603

(Received 26 October 1970)

The room-temperature ac conductivity and the real part of the dielectric constant of amorphous Se, As_2Se_3 , and As_2S_3 have been measured in the $1.0 \times 10^2 - 3.6 \times 10^{10}$ -Hz frequency range. In addition, the temperature dependence of the low-frequency dielectric constant and the ac conductivity of Se were also measured in the 320–77°K range. For all three materials the dielectric constant shows less than 15% dispersion in the entire frequency range, while the ac conductivity is proportional to ω^n with $n = 0.95 \pm 0.05$ in the $1.0 \times 10^2 - 5.0 \times 10^7$ -Hz frequency range. The results indicate that the frequency dependence of the ac conductivity may saturate below 10^{10} Hz. Consideration of different models for the frequency-dependent conductivity leads to thermally activated hopping as the most likely process. The density of the localized states participating in this process is not described adequately, however, by any of the existing theoretical treatments of amorphous materials. It is suggested that the effect of impurities and defects should be considered in detail.

I. INTRODUCTION

In recent years the successful use of some chalcogenide glasses as photoconductors in xerography, in vidicon tubes, and, most recently, their attempted use as solid-state switches, has been accompanied by substantial interest in their physical properties. The photogeneration and charge-transport mechanism were studied in detail in vitreous Se and the As-Se alloy system. In Se, photogeneration was observed to be field dependent,^{1,2} but the room-temperature transport of both electrons and holes was found to be governed by a well-defined field-independent and most likely trap-controlled drift mobility.^{3,4} In the case of As_2Se_3 however, both photogeneration and charge transport were discovered to be field dependent at room temperature.⁵ In this material, electrons were found to be localized, while holes exhibited a distribution of field-dependent mobilities. The largest mobility in this distribution was measured to be 4×10^{-5} cm²/V sec at 10^5 V/cm, which is almost 10^4 times smaller than the hole mobility in Se. As_2S_3 gave results similar to As_2Se_3 , showing hole transport only.⁶ From the structural point of view, infrared⁷ and Raman-spectroscopy⁸ studies have shown that vitreous Se consists of polymeric Se chains and

monomeric Se_8 rings, the orientations of which are random. At the same time As_2Se_3 and As_2S_3 were found to possess a network structure with complete branching between atoms.⁹ The effect on the hole and electron transport of the transition from the ring-chain structure to the complete branch structure in the As-Se alloys has been studied by Tabak¹⁰ as a function of As concentration. He was able to demonstrate that electron transport is facilitated by the Se_8 rings, while small concentrations of As are believed to act as hole traps.

At the same time the theoretical band structure of disordered systems has been developed.¹¹⁻¹⁵ The concepts which evolved are still, to some extent, speculative in view of the incompleteness of experimental results. In a solid, with translational symmetry, an abrupt drop in the density of states occurs at the edges of the conduction band at E_c , and the valence band at E_v [Fig. 1(a)]. Fluctuations in the value of the distance between lattice sites, however, result in the smearing or tailing of the band edges [Fig. 1(b)], and the localization of these tail states. The existence of a gradually decreasing density of tail states is the result of a random positional shift in the maxima and minima of the periodic potential, while localization of these states is caused by the random fluctuation in the height

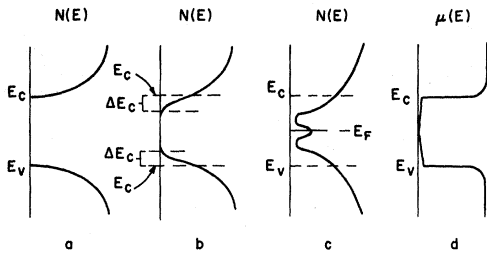


FIG. 1. Schematic representation of the density of states $N(E)$ as a function of energy (a) of crystalline materials, (b) of amorphous materials with well-defined short-range order, (c) of amorphous materials with some compositional and translational short-range order, and (d) of the mobility μ as a function of energy of amorphous materials.

of the potential maxima and minima. The extent of this tailing ΔE_c and ΔE_v has not been calculated rigorously. In these models it is assumed that the short-range order is still well defined. Structural defects, that is, changes in the local coordination number can, in fact, still occur, and these can additionally contribute to the tail states. Similarly, especially in alloys, compositional disorder can also contribute and may result in an enhanced overlap of tail states close to the center of the gap. If this happens, Davis and Mott¹⁶ assume that a narrow band of localized states will pin the Fermi level E_F between the two tails [Fig. 1(c)]. Since the original density-of-states gap has been populated by a large number of states, the original band gap has to take on new meaning. According to Mott,¹³ at the critical energies, which we shall call again E_c and E_v , the mobility of electrons and holes decreases by a factor of 100–1000 so that $E_c - E_v$ now denotes a mobility gap [Fig. 1(d)]. Within the mobility gap, carriers can move only by phonon assisted hopping between the localized states. The most often quoted evidence for the existence of localized tail states in the gap is that the drift mobility appears to be trap controlled in Se, As_2Se_3 , and As_2S_3 .^{3–6} In the Te–Se system, however, there is already evidence for a change in the drift mobility due to Te impurity states lying in the nominal band tail width.¹⁰

Additional and/or independent information about the localized states can be gained from ac conductivity measurements. Whereas normal band-type ac conductivity is mainly frequency independent up to 10^{10} – 10^{11} Hz conductivity due to hopping between localized states was shown to be proportional to ω^n , where $n \leq 1$. Pollak and Geballe¹⁷ (PG) formulated a treatment which accounts for the experimental results in the case of hopping between impurity sites. Using the method of PG, Austin and Mott¹⁵ have derived an expression for the hop-

ping conductivity assuming that it is dominated by the density of states at the Fermi level in the middle of the gap. At the same time Rockstad¹⁸ suggested that the frequency-dependent conductivity was due to hopping in the tail states located in the ΔE_c and/or ΔE_v energy range. Recent measurements on As_2Se_3 ^{19,20} and As_2S_3 ²¹ show frequency-dependent conductivity in the 10^2 – 10^5 -Hz frequency range of the type predicted by PG. At higher frequencies, however, these results indicate an even stronger frequency dependence which is interpretable in terms of hopping between states at the same energy rather than states distributed in energy. Davis and Mott¹⁶ have interpreted the results on As_2Se_3 and As_2S_3 in terms of their hopping model including states $N(E_F)$ in the middle of the mobility gap.

We report here measurements of the frequency dependence of the conductivity of Se, As_2Se_3 , and As_2S_3 in the frequency range 10^2 – 3.6×10^{10} Hz. Since the degree of disorder is much greater in the alloys the influence of glass structure upon the ac conductivity can be discussed and some insight gained into which of the proposed localized state models is most appropriate for each of the respective chalcogenide glasses. In addition, we have measured the real part of the dielectric constant ϵ' over the same frequency range, because both the real and imaginary parts of the dielectric constants are required for an unambiguous interpretation of the results. The measurements carried out in the microwave range are of special interest in that they determine whether the conductivity saturates below infrared frequencies, and so can provide an estimate of the maximum hopping frequency.

II. EXPERIMENTAL DETAILS

For the low-frequency measurements, thin films of 99.999% pure Se were evaporated at $55^\circ C$ onto aluminum, nesa glass, gold-coated glass, and gold-coated Kel-F²² substrates. The last substrate was used for temperature-dependent measurements because its thermal-expansion properties are similar to those of Se. The sample films used were in the 1–50- μ -thickness range, with thin-film (500–800 Å) gold or aluminum electrodes evaporated on them. The electrode films themselves had a sheet resistance of $\sim 1 \Omega/cm^2$. When the electrode films were thinner and presented an order of magnitude higher contact resistance, erroneous results were obtained in the 10^5 – 10^7 -Hz region. In the case of Se, the different electrode materials did not influence the experimental results. As_2Se_3 thin films were also prepared by flash evaporation on aluminum- or gold-coated glass slides. In this case the electrode material did make a difference (see Sec. III).

For the microwave-frequency measurements, Se pellets of 1.15 cm diam. were cast in sealed evacuated quartz ampoules. After casting, the slugs were sawed with a string saw into 0.18-cm-thick disks. The disks were then ground and polished so that the faces were flat and parallel to ± 0.002 cm. X-ray analysis revealed less than 5% crystallization in any of the cast Se samples. Following similar procedures, As_2Se_3 and As_2S_3 slugs were also prepared. All samples used were determined to be void free and had surfaces of optical quality.

The low-frequency measurements were made with a General Radio 1615 capacitance bridge in the 10^2 – 10^5 -Hz frequency range, and with a Boonton Q meter in the 10^5 – 5×10^7 -Hz frequency range. The microwave-frequency measurements were made at 3.6×10^{10} Hz, using a TE_{01n} cylindrical transmission cavity, which was tuned by moving the noncontacting plunger which formed the end plate, with the aid of a Lansing double-stage micro-positioner having fine-tuning graduations of 2.5×10^{-5} cm. The 1.2-cm-diam. cavity was made of copper. The cavity top and bottom were isolated from the side walls to impede surface currents in order to suppress unwanted TM modes. The suppression of the unwanted TE modes was achieved by locating the iris on the top of the cavity at the TE_{01n} -mode maxima. This resulted in 20-dB minimum mode suppression with respect to the dominant TE_{01n} modes. In the empty cavity, a $Q > 30\,000$ was achieved at room temperature. Dielectric measurements using similar cavities have been described by Horner *et al.*,²³ and we only wish to point out here that the technique requires that the samples be cut to $\sim \frac{1}{2}\lambda_d$ thickness, where λ_d is the microwave wavelength inside the sample. Under these conditions the field approaches zero at the sample surfaces, providing favorable conditions for bulk-property measurements. It is also important that the sample diameter be very close to the cavity diameter, and that the top and bottom surfaces be flat and parallel within $\pm 5\%$ of $\frac{1}{2}\lambda_d$. The former requirement ensures accurate results for the measurements of the dielectric loss, while the latter influences both the loss and dielectric-constant measurements. Low-frequency measurements were also made on all of the cast samples after the microwave measurements were completed.

III. RESULTS

A. Dielectric Constant

The dielectric constants measured for the three glasses are summarized in Table I. These results were obtained at 300 °K. In all cases we found the capacitances to be independent of the magnitude of the measuring ac field, which, field-dependence checks aside, was kept below 10^2 V/cm. No de-

TABLE I. Real part of the dielectric constant at 300 °K of Se, As_2Se_3 , and As_2S_3 at different frequencies.

Material	ϵ' at different frequencies			
	10^2 Hz	10^7 Hz	3.6×10^{10} Hz	Infrared
Se	6.36 ± 0.20	6.3 ± 0.3	6.30 ± 0.02	$(1.2 \times 10^{14} \text{ Hz})$ 6.0^a
As_2Se_3	11.2 ± 0.6	10.5 ± 0.5	9.73 ± 0.05	$(6.5 \times 10^{13} \text{ Hz})$ 9.1^b
As_2S_3	7.80 ± 0.20	7.8 ± 0.4	7.76 ± 0.02	$(20 \times 10^{12} \text{ Hz})$ 6.7^b

^aReference 28.

^bReference 29.

pendence on dc bias was observed while it was increased up to 10^5 V/cm. All measurements were conducted in the dark. At 10^2 Hz the 3% uncertainty in the results was caused mostly by errors in the sample-thickness measurements and by the non-uniformity of the sample thickness. In addition, some of the metal and Kel-F substrates were bent, which tended to exaggerate these errors. This resulted in erroneously low dielectric-constant values for some of the Se samples. The 5% error at 10^7 Hz resulted for similar reasons and, in addition, a 2% error was introduced by the limited accuracy of the Q meter itself. Unquestionably, the most precise results were obtained at microwave frequencies, where the 0.6% error was caused by klystron-frequency and cavity-dimension fluctuations.

The dielectric constant changes less than 5% in the 10^2 – 10^{10} -Hz frequency range except for As_2Se_3 , where the dispersion is 15%. In the case of Se the capacitance was found to scale with the inverse thickness $1/d$, while d was varied in the 10^{-4} – 10^{-1} -cm range. In the case of As_2Se_3 , however, the data had to be analyzed using a least-squares fit to the straight-line formula

$$C_{\text{meas}} = (\epsilon' \epsilon_0 A) (1/d) + C_s,$$

where $1/d$ is the variable and A , the area, is kept constant. This resulted in the dielectric constant shown in Table I and in surface capacitance C_s of 3.3 pF/cm^2 .

B. ac Conductivity

The ac conductivity measured at room temperature is shown in Fig. 2. For the three glasses $\sigma(\omega) \propto \omega^n$, where $0.9 < n < 1$ in the 10^2 – 10^7 -Hz frequency range. There is no evidence for the previously reported ω^2 dependence for As_2Se_3 and As_2S_3 in the 10^5 – 10^7 -Hz range.^{19–21} For As_2S_3 , reliable results could be obtained only up to 10^6 Hz because the sample impedances were too great for accurate Q -meter measurements at higher fre-

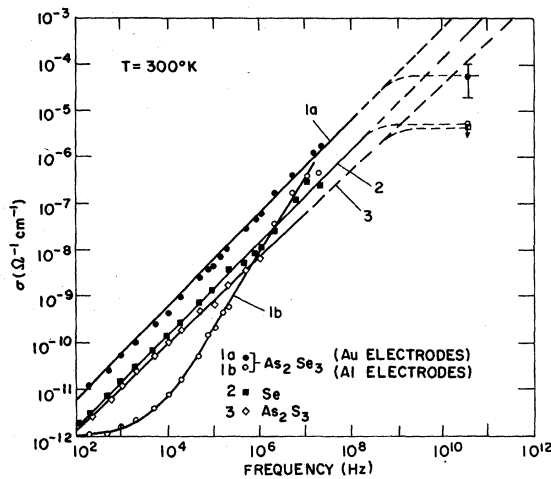


FIG. 2. Frequency dependence of the conductivity at 300°K of As_2Se_3 , Se, and As_2S_3 .

quencies.

For Se, the conductivity was found to be independent of the electrode material used and to vary about 50% over the various samples studied. On the other hand, Fig. 2 shows that at 10^2 Hz samples of As_2Se_3 with gold electrodes exhibited a factor of 10 times higher conductivity than samples with aluminum electrodes. Furthermore, the measured parallel conductance was found to scale with thickness when gold electrodes were deposited on As_2Se_3 , but did not scale when aluminum electrodes were employed. Thus it is concluded that curve 1a in Fig. 2 represents the true ac conductivity of As_2Se_3 .

Figure 2 also shows the conductivity of As_2Se_3 at 3.6×10^{10} Hz, and the upper limit placed on the conductivity of Se and As_2S_3 at that frequency. The sensitivity of the microwave cavity was such that measurements of dielectric loss could only be carried out for $\tan \delta \geq 3 \times 10^{-4}$. This translates into a minimum sample conductivity of $5 \times 10^{-6} \Omega^{-1} \text{cm}^{-1}$ for the three glasses in question. The experimental results indicated that for Se and As_2S_3 the conductivity was either just at or below this measurement threshold. This means that a linear extrapolation of the low-frequency conductivity to 10^{10} Hz would have to result in a value well above the measured microwave conductivity.

The temperature dependence of the ac conductivity of Se was measured in the 320–77°K range. The results obtained for a typical sample are shown in Fig. 3, where $\log \sigma$ is plotted as a function of $1/T$. The figure also shows the dc conductivity measured for this sample at 300°K. The straight line drawn through the dc value has a slope of 0.95 eV which is the dc conductivity activation energy reported previously.⁴ At room temperatures

the dc conductivity is two orders of magnitude lower than the ac conductivity at 10^2 Hz. As the temperature is increased the ac conductivity seems to approach the dc conductivity asymptotically at all frequencies. Consequently the frequency dependence decreases with increasing temperature as shown in Fig. 4, i. e., at 320°K, $\sigma(\omega) \propto \omega^{0.85}$, while at 77°K, $\sigma(\omega) \propto \omega^{1.08}$. Similar results were obtained on other Se samples tested; however, the exponent was found to vary ± 0.05 among the different samples at a given temperature. The temperature dependence of the ac conductivity of As_2Se_3 ^{19,20} and As_2S_3 ²¹ has been measured previously and the results are similar to our results on Se.

IV. DISCUSSION OF RESULTS

A. Dielectric Constant

A number of researchers did measure the microwave dielectric constant of vitreous Se previously, but for As_2Se_3 and As_2S_3 we could find no published data at 10^{10} Hz. In the case of Se, the earlier measurements summarized by Eckart and Rabenhorst²⁴ were done at 1.0×10^{10} Hz and at 2.5×10^{10} Hz; the

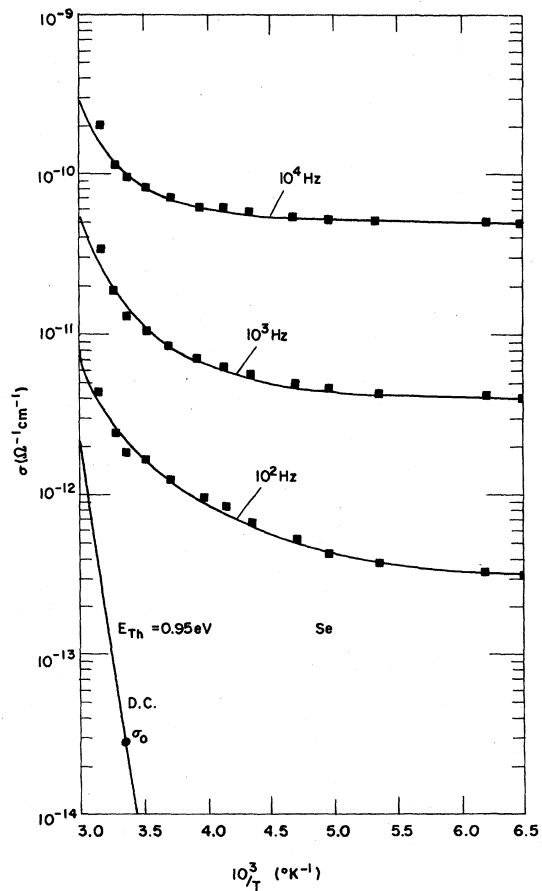


FIG. 3. Semilog plots of the conductivity vs reciprocal temperature for Se, at different frequencies.

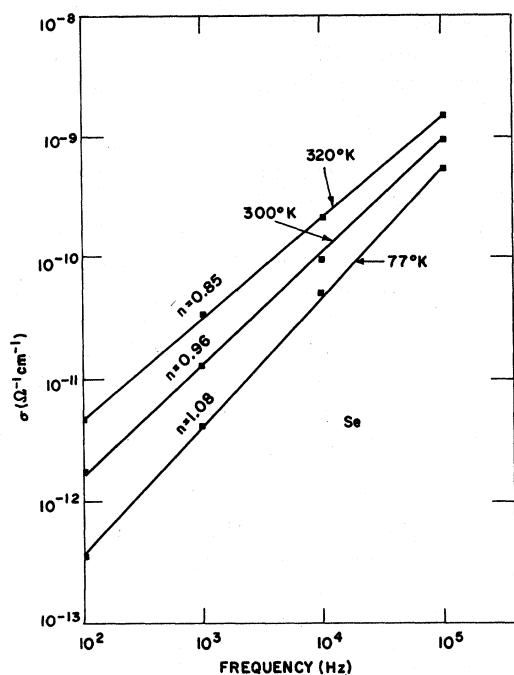


FIG. 4. Frequency dependence of the conductivity of Se at different temperatures.

reported values are in the $\epsilon' = 6.0-6.6$ range. There is no systematic difference between the results at the two frequencies. Our measurements at 3.6×10^{10} Hz resulted in $\epsilon' = 6.30 \pm 0.02$ which is in the middle of the range. The wide spread in the values of ϵ' reported in the literature is probably caused by incorrect estimation of cavity or waveguide filling factors. This would tend to reduce the measured ϵ' . In addition, any partial crystallization of the samples would tend to increase the measured ϵ' . With the large cross-sectional samples used in our technique, the first source of errors was minimized, while x-ray analysis revealed less than 5% crystallization. In addition, the dark dc conductivity measured to be $10^{-14} \Omega^{-1} \text{cm}^{-1}$ is appropriate for amorphous Se. At low frequencies only two values have been reported earlier, $\epsilon' = 6.0$ in the range $10^2-3 \times 10^9$ Hz by von Hippel,²⁴ and $\epsilon' = 6.3 \pm 0.1$ in the range $5 \times 10^4-4 \times 10^6$ Hz by Clark and Reading.²⁴ Our work resulted in $\epsilon' = 6.36 \pm 0.20$ at 10^2 Hz. This means that there is less than 2% dispersion in ϵ' between 10^2 and 3.6×10^{10} Hz. This eliminates any possibility of significant dielectric relaxation or resonance in this frequency range due to interfacial polarization or permanent dipoles. Furthermore, underlining this conclusion, we found that ϵ' (10^2-10^5 Hz) decreased by less than 2% as the temperature was decreased from 320 to 77 °K.

For the case of As_2S_3 , Owen and Robertson²¹ report a dielectric constant $\epsilon' = 9.5$ at 10^5 Hz which

decreases to $\epsilon' = 6.5$ at 5×10^9 Hz. This dispersion is accompanied by a temperature-independent ω^2 dependence of the ac conductivity in this frequency range. As Table I shows, we did not measure such a change in the dielectric constant, so that at 3.6×10^{10} Hz we obtained a value of $\epsilon' = 7.75 \pm 0.2$, while at 10^2 Hz we found $\epsilon' = 7.80 \pm 0.2$.

For As_2Se_3 , Kolomiets²⁵ reported a dielectric constant of 12.25 at 10^5 Hz. Our measurements yielded $\epsilon' = 9.73 \pm 0.05$ at 3.6×10^{10} Hz and $\epsilon' = 11.2 \pm 0.5$ at 10^2 Hz, giving a change of 15%. As already described in Sec. II, the low-frequency dielectric constant was obtained using a least-squares fit of the data taking $1/d$ as the linear variable. The surface capacitance C_s obtained by this procedure is due either to the bending of the bands at the metal- As_2Se_3 interface or to surface states. The former should exhibit a field-dependent character which was not observed. It is more likely, therefore, that C_s arises from surface states. Leiga has observed that the photoemission threshold of As_2Se_3 depends on the aging time of the sample surface,²⁶ while Berkes and Hillegas have found that at room ambient conditions, an oxide layer may form on the surface.²⁷ Since all our samples were aged between deposition and electrode evaporation, it is likely that they developed surfaces rich in surface states.

Table I also shows the dielectric constant of the three glasses measured at infrared frequencies,^{28,29} which are 5-16% lower than those measured at microwave frequencies. Therefore we predict strong infrared absorption in the far infrared for all three glasses. The variation in dielectric constant in this frequency range is larger for the alloys than for Se. Therefore the far-infrared absorption may be associated with the degree of disorder in these systems.

B. ac Conductivity

Frequency-dependent ac conductivity in the 10^2-10^8 -Hz range has been observed previously for a wide variety of low-mobility insulators: oxides, organic materials, and chalcogenide glasses. For As_2Se_3 the measurements of Owen¹⁹ and Kitao *et al.*,²⁰ and for As_2S_3 the results of Owen and Robertson,²¹ can best be described by the experimental formula

$$\sigma(\omega) = \sigma_0 + \sigma_1, \quad (1)$$

where σ_0 is the dc conductivity and σ_1 is an additional frequency-dependent conductivity given by

$$\sigma_1 = A\omega^n, \quad (2)$$

where A is a constant and $0.8 \leq n \leq 1$ at room temperature. The range of values given for n ap-

plies in the 10^2 – 10^5 -Hz frequency range in the references cited above. At higher frequencies, $n \approx 2$ is reported^{19–21} and we shall call this the ω^2 -dependence region. In the 10^2 – 10^5 -Hz frequency range, σ_1 was observed to be temperature dependent, while the ω^2 term was found to be temperature independent. Shaw has suggested that the ω^2 dependence is the result of the relatively small but finite resistances³⁰ created by the thin-film contacts. Since some of our Se samples did exhibit this type of behavior we carried out an analysis as follows: The three-component equivalent network shown on Fig. 5 can be used to describe the experimental situation, where R_b and C_b are the parallel resistance and capacitance of the bulk sample, and R_c is the resistance of the contacts in series with the sample. For this network we obtain the following expressions for the parallel conductance and capacitance as a function of frequency:

$$G_p = \frac{1}{R_b} \left(\frac{(1 + R_c/R_b) + \omega^2 R_c R_b C_b^2}{(1 + R_c/R_b)^2 + \omega^2 R_c^2 C_b^2} \right), \quad (3)$$

$$C_p = C_b \left(\frac{1}{(1 + R_c/R_b)^2 + \omega^2 R_c^2 C_b^2} \right). \quad (4)$$

For simplicity let us assume first that R_b is frequency independent, and that $R_c/R_b \ll 1$. In this case, $G_p \approx 1/R_b$ up to frequency $\omega_1 = [(R_c R_b)^{1/2} C_b]^{-1}$. Clearly, the larger R_b is, the smaller ω_1 becomes. Therefore the effect of the contact resistances is most crucial for highly insulating materials. At frequency $\omega_2 = (R_c C_b)^{-1}$, G_p saturates at the value $1/R_c$. Between ω_1 and ω_2 , G_p is proportional to ω^2 . If R_b is itself frequency dependent, Eqs. (3) and (4) are still useful provided $R_b \propto \omega^{-n}$, where $n < 2$.

Using the above model we calculated the electrode resistances to be in the range 1–10 Ω/cm^2 for the Se samples which exhibited the ω^2 dependence. Artificial contact resistances R_c were introduced in the form of series resistors in the measuring circuit, and the measured G_p and C_p 's were then found to satisfy Eqs. (3) and (4). Starting at $10^3 \Omega$, the value of R_c was reduced until its effect could not be observed in the measurements. By this technique we arrived at the same values as those calculated for the resistance of the evaporated electrodes. Curves 1a, 2, and 3 in Fig. 2 were obtained with thick ($> 500 \text{ \AA}$) electrodes where

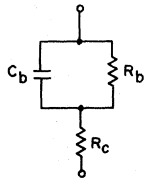


FIG. 5. Schematic representation of the electroded sample as used in the low-frequency ac measurements.

sheet resistance was $\sim 1 \Omega/\text{cm}^2$ and no ω^2 dependence was observed. Curve 1b, however, clearly illustrates this contact limitation, and the blocking nature of aluminum contacts on As_2Se_3 . In Sec. II we indicated that gold electrodes formed Ohmic contacts on As_2Se_3 while aluminum electrodes were blocking. A comparison of curves 1a and 1b obtained for the same sample reveals that aluminum contacts reduced the conductance of this sample by a factor of 6 at 10^2 Hz. The depleted sample has a relatively frequency-independent conductance up to 10^3 Hz. Due to the increased sample resistance, ω_1 was lowest for the depleted sample. Therefore, starting at 5×10^3 Hz, $\sigma(\omega) \propto \omega^2$, and the contact resistances dominated the result even though they were not higher than those for which gold contacts were used (curve 1a). It should be remarked here that a final check of the electrode-resistance limitation can be made by measuring C_p above ω_2 . As Eq. (4) shows, it drops to zero as ω^{-2} . We have not been able to observe this with our evaporated electrodes because ω_2 was always above 10^8 Hz.

An additional indication that the previously reported ω^2 dependences^{19–21} are due to contact resistance results from measurement of the ac conductivity at microwave frequencies, when contacts are not used. Both, our results at 3.6×10^{10} Hz and those of Taylor *et al.*³¹ at 10^9 Hz show that the magnitude of the conductivity at microwave frequencies is below that obtained from bridge measurements at 2.5×10^8 Hz.¹⁹ Since ϵ' changes less than 1% over this frequency interval, these results cannot be explained in terms of a resonance-type dielectric dispersion.

For all three solids, the room-temperature dc conductivity σ_0 is at least a factor of 10 below $\sigma(\omega)$ at 10^2 Hz. Therefore $\sigma(\omega) \approx \sigma_1$, so that in the 10^2 – 10^7 -Hz frequency range, $\sigma(\omega) \propto \omega^n$, where $n \leq 1$; Fig. 2 demonstrates that the microwave-frequency conductivity lies below the straight-line extension of the low-frequency conductivity for all three glasses. This means that σ_1 must saturate in the 10^7 – 10^{10} -Hz frequency interval. Experiments were conducted in this frequency range on As_2Se_3 by Taylor *et al.*³¹ In Fig. 6 we have reproduced the data points from curve 1a of Fig. 2 and have included the results at 10^9 Hz in addition to the data point at 3.6×10^{10} Hz. The best straight line through all the experimental points with a slope of ≈ 1 (line 1) yields a value for conductivity a factor of 2.5 above the experimental value at 10^9 Hz, and is almost two orders of magnitude above the conductivity at 3.6×10^{10} Hz. If we assume, however, that the results of Taylor *et al.*³¹ lie on a linear extension of the low-frequency data, line 2 can be drawn. This line has a slope of 0.92. Although measurements of the low-frequency conductivity lie along this line, conductivities measured above

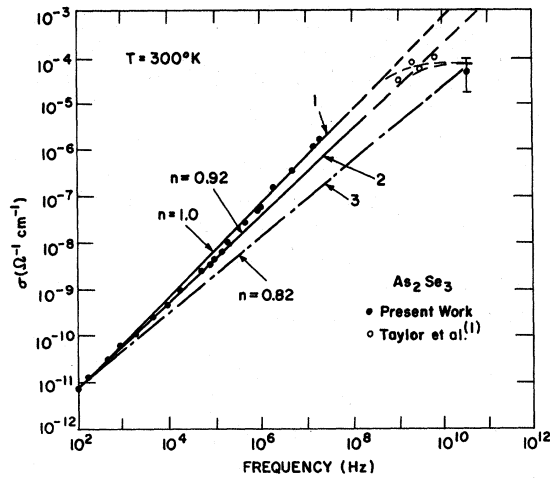


FIG. 6. Frequency dependence of the conductivity at 300°K of As_2Se_3 .

10^5 Hz lie 20–30% above it. Even in this case the conductivity at 3.6×10^{10} Hz lies about a factor of 10 below line 2. Line 3 with a slope of 0.82 connecting the results at 10^2 Hz and at 3.6×10^{10} Hz does not fit the data at all. Therefore we conclude that σ_1 saturates at 10^9 – 10^{10} Hz. Similarly, saturation takes place for Se and As_2S_3 at the same frequencies (see Fig. 2).

The real and imaginary parts of the complex dielectric constant are related to each other through the Kramers-Kronig relations. When σ_1 has a power-law dependence on ω , ϵ'_1 the corresponding contribution to ϵ' is given by¹⁸

$$\epsilon'_1 = (\sigma_1 / \omega \epsilon_0) \tan \frac{1}{2} \pi n. \quad (5)$$

For all three glasses the measured dielectric constant and conductivity were found to satisfy Eq. (5).

The salient features in the temperature dependence, Fig. 3, are (a) the dc conductivity is approached at high temperatures at all frequencies; (b) as the temperature is decreased, the temperature dependence of $\sigma(\omega)$ decreases until at 77°K the activation energy becomes too small to be measured accurately; and (c) as shown in Fig. 4, $\sigma(\omega) \propto \omega^n$ at all temperatures and the value of n increases with decreasing temperature. The same features were observed in the temperature dependence of $\sigma(\omega)$ for As_2Se_3 ¹⁹ and As_2S_3 .²⁰ For Se at low temperatures the activation energy for ac conductivity is much lower than the activation energy of the dc conductivity or the activation energy of the hole or electron mobilities.

C. Models for ac Conductivity

ac conductivity is proportional to the out-of-phase part of the polarization produced by an electric

field applied to the solid. In the case of high-mobility ($> 10 \text{ cm}^2/\text{V sec}$) wide-band solids when the conductivity is dominated by thermally excited carriers in the band, the ac conductivity is frequency independent to a first approximation, up to microwave frequencies. At very low temperatures, when isolated impurity states can dominate the conductivity of these materials, a frequency-dependent conductivity is observed¹⁷ with temperature dependence as shown in Figs. 3 and 4.

In the case of the low-mobility chalcogenides investigated in this work, the following processes could conceivably influence the observed ac conductivity: (i) interfacial polarization (Maxwell-Wagner type), (ii) Schottky barriers at the metal-glass interface, (iii) space-charge limited currents, (iv) hopping-type conduction between localized states which may be tail states or states at the middle of the gap [$N(E_F)$], (v) trap-controlled conduction. Interfacial polarization³² can be eliminated because the glasses do not exhibit any microstructure and because the decreasing temperature dependence of $\sigma(\omega)$ is not expected on this basis. Process (ii), involving Schottky barriers originating at the metal-glass interface has been treated recently by Simmons *et al.*³³ They predict a temperature-independent activation energy and in addition predict a temperature-dependent capacitance. Se, As_2Se_3 , and As_2S_3 all show a decrease in activation energy with decreasing temperature. In addition, Se did not show a temperature-dependent capacitance. In process (iii) the space-charge-limited currents would be strongly field dependent and therefore the ac conductance would be expected to show field dependence.³⁴ The lack of field dependence in the measured σ_1 for chalcogenides suggests that this process does not apply below 10^5 V/cm. We now consider the differences in the effect on σ_1 , of the two types of states involved in process (iv).

We should note, at the outset, that the hopping theory of PG does describe most of the observed phenomena in σ_1 . PG have shown that if hopping takes place between a random distribution of localized states, then $\sigma_1 \propto \omega^n$ [using the notation of Eq. (1)], where $0.5 < n < 1$, the lower value of n occurs for multiple hops while the higher value occurs for single hops. If hopping takes place between identical sites, then $n = 2$ when $\omega < \tau^{-1}$, the characteristic hopping frequency. Since the hopping process is phonon assisted, a small but finite temperature dependence in σ_1 should exist even at low temperatures. In addition, according to Pollak,³⁵ at higher temperature, multiple hops occur frequently, while at low temperature, single hops predominate. This leads to an increased thermal activation at high temperatures, with a corresponding decrease in the frequency dependence.

Our results for Se satisfy all the major predictions of the theory for randomly distributed hopping states, with the single exception that at low temperatures the experimentally measured exponent is > 1.0 . This can only be accounted for if we assume that there are a finite number of identical centers and hopping between them does contribute to σ_1 especially at low temperatures. Using our measurements and the results of temperature-dependent studies of Owen¹⁹ and Owen and Robertson,²¹ similar statements can be made about As_2Se_3 and As_2S_3 .

Rockstad¹⁸ has found that in the case of As_2Te_3 and Te_2AsSi , the ratio of σ_0/σ_1 was always constant at 300 °K when σ_1 was measured at 10^5 – 10^6 Hz, and σ_0 varied by a factor of 100 for the various alloy compositions measured. On the basis of this observation, assuming that σ_1 is a measure of thermally activated intrinsic-carrier generation, it is suggested that the constancy of the ratio indicates that regular tail states (those near the band edges) are involved in the hopping process. In Table II, we have summarized our room-temperature dc and ac measurements at 10^4 Hz. This is a frequency at which $\sigma_1 \approx \sigma(\omega)$, but the contact resistances do not yet influence the results. The table shows the calculated ratios σ_0/σ_1 . The ratios differ by a factor of 10^3 among the chalcogenides we measured. In fact, while σ_0 is a factor of 10^2 larger for As_2Se_3 than for As_2S_3 , σ_1 at 10^4 Hz is only a factor of 5 larger for the selenide. On the basis of structural studies As_2Se_3 and As_2S_3 are known to possess a comparable degree of disorder. It is reasonable to expect As_2Se_3 and As_2S_3 to exhibit similar functional dependence of the density of states $N(E)$ in the band tails. On the basis of our measurements we infer that the density of states responsible for σ_1 , the ac hopping conductivity, does not depend on the thermal activation energy of σ_0 . We presume, therefore, that it is unlikely that the states influencing the hopping conductivity are regular tail states. Comparison with Se leads to the same conclusion.

Let us consider states of type *b* [see Fig. 1(b)]. Using the theory of PG, Austin and Mott¹⁵ derived

a theoretical formula for σ_1 which is proportional to $[N(E_F)]^2$, the density of states at the Fermi level, close to the middle of the mobility gap. They assume that the frequency-dependent ac conductivity of As_2Se_3 ¹⁹ and As_2S_3 ²¹ is evidence for the existence of a density of states $N(E_F) \sim 10^{18} \text{ cm}^{-3}$. They conclude that this band of compensated states pins the Fermi level near the middle of the gap, and that $N(E_F)$ increases with decreasing mobility gap, due to the greater overlap of tail states. $N(E_F)$ also is predicted to increase with increasing disorder. On the basis of our results, however, a decrease of 0.60 eV in the band gap (see Table II) causes an increase of less than a factor of 2.5 in $N(E_F)$ when we compare As_2Se_3 and As_2S_3 .^{30,36} For Se, $N(E_F)$ is expected to be small because the degree of disorder in this material is less than in the alloys. The Austin-Mott¹⁵ model applied to our data would predict a larger value for $N(E_F)$ in Se than As_2S_3 . This is puzzling especially in view of the results of the internal photoemission measurements carried out on a series of metals and amorphous Se.³⁷ These measurements clearly showed that the Fermi level is not pinned at the metal-Se interface by surface, band, or mobility-gap states in Se. In addition, the effective band gap was found to be 2.2 eV which, when compared with the 2.4-eV photoconductivity gap, indicates that the width of the tail states which can contribute to charge transport is ~ 0.1 eV. Davis and Mott came to similar conclusions about the width of the tail states.¹⁶ On the basis of the photoinjection results it is unlikely that the tail states do overlap in Se, and experimentally it was observed that even if they do, their density is too small to pin the Fermi level. Consequently, we believe they cannot be responsible for the ac hopping conductance. In the case of As_2Se_3 , the curves 1a and 1b in Fig. 2 show that different metals can form different types of contacts with this glass. This again indicates that the Fermi level is not pinned by $N(E_F)$ and, therefore, does not control σ_1 . We have no evidence for blocking contact on As_2S_3 which seems to have the highest intrinsic resistivity among the three chalcogenides measured, but since the degree of disorder is the same as in As_2Se_3 , here too we do not expect a large density of $N(E_F)$.

Therefore it appears that either the model of hopping between states of type *a* and *b* is itself inadequate, or that the hopping occurs between states of yet another type. We suggest that impurity states and defect states ought to be considered in detail. Cohen³⁸ has briefly described the nature of such states in amorphous materials; however, detailed calculations predicting their density as a function of energy have not been reported. The influence of dopants on the electrical properties of Se has been investigated by Tabak¹⁰

TABLE II. dc conductivity, ac conductivity at 10^4 Hz, and optical band gap at 300 °K of Se, As_2Se_3 , and As_2S_3 .

Material	Conductivity (at 300 °K)			Optical band gap E_G (eV)
	σ_0 ($\Omega^{-1} \text{ cm}^{-1}$)	σ_1 (10^4 Hz) ($\Omega^{-1} \text{ cm}^{-1}$)	σ_0/σ_1	
Se	2.8×10^{-14}	1.5×10^{-10}	1.8×10^{-4}	2.00 ^a
As_2Se_3	1.0×10^{-12}	6.0×10^{-10}	1.6×10^{-1}	1.74 ^b
As_2S_3	5.0×10^{-15}	1.1×10^{-10}	4.6×10^{-5}	2.32 ^b

^aReference 36.

^bReference 29.

and more recently by Lacourse *et al.*³⁹ Tabak has studied in detail the influence of small percentages of As in Se. He found that 0.5% As does not change the optical or photoconductivity gap of Se. Yet we find that it does increase ac conductivity by a factor of 5 above the value in Table II without substantial increase in σ_0 . This is a preliminary result and further experiments are planned.

The last of the processes enumerated is trap-controlled conduction which has been discussed by Spear,³ by Hartke,⁴ and most recently by Tabak⁴⁰ in connection with the drift mobility of photogenerated carriers in Se. These authors have not, however, considered the influence of this process on the ac conductivity. For the case of trap-controlled ac conductivity carriers are thermally excited from traps into the extended states and subsequently retrapped. For a single trap level this would lead to a single relaxation frequency manifested by an ω^2 dependence of σ in the vicinity at this relaxation frequency. For a distribution of trap levels, however, the exact form of the frequency dependence of σ should depend on the detailed nature of the distribution. To our knowledge this problem has not yet been treated.

V. SUMMARY

From the measurement of the dielectric constant and ac conductivity of Se, As_2Se_3 , and As_2S_3 , the following results and conclusions were obtained:

(a) A precise value of the dielectric constant was determined at 3.6×10^{10} Hz and compared with the less precise lower-frequency results and published values at infrared frequencies. There is very little dispersion in the 10^2 – 10^{10} -Hz frequency range for all three glasses. The results predict a more rapid dispersion accompanied by absorp-

tion in the far-infrared frequency range.

(b) At room temperature, and below, the ac conductivity of these chalcogenides varies as ω^n in the 10^2 – 10^7 -Hz frequency range. At 300 °K, $n = 0.95 \pm 0.05$ for all three glasses, and increases at lower temperatures. The results indicate that this frequency dependence may saturate below 10^{10} Hz.

(c) Even though Se is a two-carrier system in which, at temperatures above 100 °K, dc conductivity is characterized by well-defined trap-controlled drift mobility, it exhibited the same type of ac conductivity as As_2Se_3 and As_2S_3 , both of which are one-carrier systems with a distribution of field-dependent drift mobilities. Therefore it seems that the ac conductivity of these materials is not a particularly sensitive measure of variation in the band or mobility gap.

The observed frequency-dependent conductivity can best be described by a thermally activated hopping model. The relative insensitivity of the ac conductivity to the band or mobility gap suggests that localized states generated by impurities or structural defects affecting the short-range order may be important, and their role in amorphous chalcogenides should be considered in detail theoretically and experimentally.

ACKNOWLEDGMENTS

The authors wish to thank S. Ing, M. Scharfe, H. Scher, M. Tabak, and A. Ward for many useful discussions, and R. F. Shaw for his helpful comments on ac measurements. We also wish to thank S. Ing, P. Nielsen, and M. Tabak for providing us with samples. A special thanks to M. Winchell for building for us an excellent microwave cavity.

¹M. D. Tabak and P. J. Warter, Jr., *Phys. Rev.* **173**, 899 (1968).

²D. Pai and S. W. Ing, Jr., *Phys. Rev.* **173**, 729 (1968).

³W. E. Spear, *Proc. Phys. Soc. (London)* **B70**, 699 (1957); **B76**, 826 (1960).

⁴J. L. Hartke, *Phys. Rev.* **125**, 1177 (1962).

⁵M. E. Scharfe, *Phys. Rev.* (to be published).

⁶S. W. Ing, Jr., J. H. Neyhart, and F. Schmidlin, *J. Appl. Phys.* (to be published).

⁷G. Lucovsky, A. Mooradian, W. Taylor, G. B. Wright, and R. C. Keezer, *Solid State Commun.* **5**, 113 (1967).

⁸A. Mooradian and C. B. Wright, *Phys. Rev. Letters* **16**, 999 (1966).

⁹M. B. Myers and E. J. Felty, *Mater. Res. Bull.* **2**, 535 (1967).

¹⁰M. D. Tabak, *J. Phys. Chem. Solids* (to be published); J. Schottmiller, M. Tabak, G. Lucovsky, and A. Ward, *Non-Cryst. Solids* **4**, 80 (1970).

¹¹L. Banyai, in *Proceedings of the International Con-*

ference on the Physics of Semiconductors, Paris, 1964 (Dunod, Paris, 1964), p. 417.

¹²A. I. Gubanov, *Quantum Electron Theory of Amorphous Conductors* (Consultants Bureau, New York, 1965).

¹³N. F. Mott, *Advan. Phys.* **16**, 49 (1967); *Phil. Mag.* **17**, 1259 (1968); *J. Non-Cryst. Solids* **1**, 1 (1968); *Phil. Mag. Suppl.* **19**, 35 (1969).

¹⁴M. H. Cohen, M. Fritzsche, and S. R. Ovshinsky, *Phys. Rev. Letters* **22**, 1065 (1969).

¹⁵I. G. Austin and N. F. Mott, *Advan. Phys.* **18**, 41 (1969).

¹⁶E. A. Davis and N. F. Mott, *Phil. Mag.* (to be published).

¹⁷M. Pollak and T. H. Geballe, *Phys. Rev.* **122**, 1742 (1961).

¹⁸H. K. Rockstad, *Solid State Commun.* **7**, 1507 (1969); *J. Non-Cryst. Solids* **2**, 224 (1970).

¹⁹A. E. Owen, *Glass Ind.* **48**, 637 (1967).

²⁰M. Kitao, F. Araki, and S. Yamada, *Phys. Status Solidi* **37**, K119 (1970).

²¹A. E. Owen and J. M. Robertson, *J. Non-Cryst.*

Solids 2, 40 (1970).

²²Trademark of the Fluorocarbon Co., Pine Brook, N. J. 07058.

²³F. Horner, T. A. Taylor, R. Dunsmuir, J. Lamb, and W. Jackson, Proc. IEEE 93, 11153 (1946).

²⁴F. Eckart and H. Rabenhorst, Ann. Physik 19, 381 (1956).

²⁵B. T. Kolomiets, Phys. Status Solidi 7, 713 (1964).

²⁶A. Leiga (unpublished).

²⁷J. S. Berkes and J. Hillegas (private communication).

²⁸T. J. Dowd, Proc. Phys. Soc. (London) 64, 783 (1951).

²⁹E. J. Felty, G. Lucovsky, and M. B. Myers, Solid State Commun. 5, 555 (1967).

³⁰R. F. Shaw (private communication).

³¹P. C. Taylor, G. A. Bishop, and D. L. Miller, in International Conference on the Physics of Semiconduc-

tors, Boston, 1970 (unpublished).

³²L. K. H. VanBeek, Progr. Dielectrics 7, 69 (1967).

³³J. A. Simmons, G. S. Nadkarin, and M. C. Lancaster, J. Appl. Phys. 41, 588 (1970).

³⁴B. Binggeli and M. Kiess, J. Appl. Phys. 38, N984 (1967).

³⁵M. Pollak, Phys. Rev. 138, A1822 (1965).

³⁶J. L. Hartke and P. J. Regensburger, Phys. Rev. 139, A970 (1965).

³⁷A. I. Lakatos and J. Mort, Bull. Am. Phys. Soc. 14, 737 (1969); J. Mort and A. I. Lakatos, J. Non-Cryst. Solids 4, 391 (1970).

³⁸M. H. Cohen, J. Non-Cryst. Solids 4, 391 (1970).

³⁹W. L. Lacourse, V. A. Twaddell, and J. D. Mackenzie, J. Non-Cryst. Solids 3, 234 (1970).

⁴⁰M. D. Tabak, Phys. Rev. B 2, 2104 (1970).

Analysis of the Grüneisen Parameter for Cu and Associated Force-Model Calculations for Cu and Ag

Joseph L. Feldman and Earl F. Skelton

U. S. Naval Research Laboratory, Washington, D. C. 20390

(Received 26 October 1970)

An analysis of the temperature dependence of the thermodynamic Grüneisen parameter γ_1 of Cu is performed in order to obtain the values of $\gamma_D(n)$, essentially the volume derivatives of the n th moments of the phonon spectrum. Simple phenomenological force-model calculations of $\gamma_1(T)$ and $\gamma_D(n)$, which principally make use of the pressure derivatives of the elastic constants and published "harmonic" force models obtained from neutron-diffraction data, have also been performed for Cu and Ag. The sensitivity of the results of the force-model calculations to the various quoted values of the second-order force constants and the pressure derivatives of the elastic constants is indicated. Comparison is made with experiment wherever possible.

INTRODUCTION

As discussed by Barron *et al.*,¹ an appropriate analysis, based on the quasiharmonic approximation, of the thermodynamic Grüneisen parameter $\gamma_1(T)$, yields information about the volume dependences of several moments of the vibrational frequency distribution. It seemed worthwhile to perform this analysis for Cu,² although the temperature dependence of γ_1 for Cu is somewhat weaker than it is for substances used in previous analyses.³ We point out that these types of analyses may be useful for accurately determining volume dependences of the Debye-Waller factor or specific heat, since in the quasiharmonic approximation these quantities are describable in terms of moments of the frequency spectrum over wide temperature regions. Partly for the purpose of comparison with our analysis for Cu, we have also performed related calculations based on simple phenomenological force models appropriate to Cu and Ag.

A theoretical evaluation of $\gamma_1(T)$, in the quasi-harmonic approximation, chiefly requires a knowledge of second-order force constants and their volume dependences. Very recently Sharma and Singh⁴ have presented results of calculations of $\gamma_1(T)$ for the noble metals based on the Chéveau model,⁵ which explicitly takes into account the electron-gas contribution to the force constants in an approximate way. The potential parameters involved in their calculations were determined according to the method of long waves, using the measured values of the adiabatic elastic constants at each temperature of interest and the pressure derivatives of these constants at room temperature. We have performed similar force-model calculations of both $\gamma_1(T)$ and $\gamma_D(n)$, essentially the volume derivative of the n th moment of the frequency distribution. Our model involves published second-order force constants determined from neutron data⁶⁻⁸ and the assumption that the volume derivatives of further than nearest-neighbor force constants can be neglected. The